Photonic crystal fabrication in lithium niobate via pattern transfer through wet and dry etched chromium mask

Ozgur Yavuzcetin, Herman P. Novikov, Rebecca L. Dally, Sean T. Malley, Nicholas R. Perry et al.

1. REPORT DATE **OCT 2012**	2. REPORT TYPE	3. DATES COVERED **00-00-2012 to 00-00-2012**

4. TITLE AND SUBTITLE	5a. CONTRACT NUMBER
Photonic crystal fabrication in lithium niobate via pattern transfer through wet and dry etched chromium mask	5b. GRANT NUMBER
	5c. PROGRAM ELEMENT NUMBER
6. AUTHOR(S)	5d. PROJECT NUMBER
	5e. TASK NUMBER
	5f. WORK UNIT NUMBER

7. PERFORMING ORGANIZATION NAME(S) AND ADDRESS(ES) **Northeastern University,Electronic Materials Research Institute and Department of Physics,Boston,MA,02115**	8. PERFORMING ORGANIZATION REPORT NUMBER

9. SPONSORING/MONITORING AGENCY NAME(S) AND ADDRESS(ES)	10. SPONSOR/MONITOR'S ACRONYM(S)
	11. SPONSOR/MONITOR'S REPORT NUMBER(S)

12. DISTRIBUTION/AVAILABILITY STATEMENT **Approved for public release; distribution unlimited**

13. SUPPLEMENTARY NOTES

14. ABSTRACT

15. SUBJECT TERMS

16. SECURITY CLASSIFICATION OF:			17. LIMITATION OF ABSTRACT	18. NUMBER OF PAGES	19a. NAME OF RESPONSIBLE PERSON
a. REPORT **unclassified**	b. ABSTRACT **unclassified**	c. THIS PAGE **unclassified**	**Same as Report (SAR)**	**7**	

Photonic crystal fabrication in lithium niobate via pattern transfer through wet and dry etched chromium mask

Ozgur Yavuzcetin,[a] Herman P. Novikov, Rebecca L. Dally, Sean T. Malley, Nicholas R. Perry, Birol Ozturk, and Srinivas Sridhar
Electronic Materials Research Institute and Department of Physics, Northeastern University, Boston, Massachusetts 02115, USA

The need to fabricate photonic crystals from lithium niobate (LN) with accurate feature sizes is important to the development of optoelectronic devices. This paper reports a fabrication process to dry etch X-cut LN at a submicron scale using electron beam lithography and chromium as a hard mask. The chromium mask was used for both dry-etching and wet-etching in a unique method. Problems and solutions found during fabrication are presented. Arrays consisting of 400 nm diameter holes with a high aspect ratio were etched in LN, creating photonic crystals modeled to transmit light in the infrared spectrum. © *2012 American Institute of Physics*. [http://dx.doi.org/10.1063/1.4756958]

I. INTRODUCTION

Lithium niobate (LN) is among the most prevalent materials used in integrated optical devices, mainly guided-wave optics,[1,2] due to a variety of favorable optical properties. The material is birefringent by nature and characterized by high linear electro-optic, photoelastic, piezoelectric, and pyroelectric coefficients. In combination, these properties can lead to significant refractive index changes if the material is optically stimulated.[3]

Advancements in fabrication equipment have enabled the integration of photonic crystal structures in LN, opening the door for the realization of novel optical devices. Photonic crystal structures affect the propagation of electromagnetic waves through the base material, allowing certain wavelengths that collectively form bands to pass through. Other sets of wavelengths, known as band gaps, are blocked, allowing for selective transmission of light depending on the desired application.

Production of photonic crystals in −X-cut LN requires efficient and reliable fabrication techniques on a sub-micron scale. To date, most photonic crystal fabrication has been done using focused ion beam (FIB) and ion beam enhanced etching (IBEE) methods.[4–6] Alternative methods such as reactive ion etching (RIE) have proven to be difficult since LN is very dry-etch resistant and due to re-deposition of LiF during the etching process.[7,8]

In fabrication of dry-etched LN photonic crystals, the fabrication methods can be summarized as the following: application of photoresist to the −X-cut face of the LN surface, electron beam (e-beam) lithography and development, and wet (chemical) or dry (plasma) etching of the LN crystal. The etching is usually a two-stage process requiring an initial hard mask on the surface of the crystal and is the most difficult step in fabrication. This report describes some of the processes developed for improved fabrication of photonic crystal nanostructures in −X-cut LN crystals. Here, we are presenting two ways of etching hard mask (Cr) at sub-micron scales. Our

results show that wet etching of Cr hard mask can be applied at this size scales.

II. DESIGN

In order to utilize the fabricated photonic crystal device in device applications, the photonic crystal parameters should be tailored such that the photonic band gap occurs in the desired range of wavelengths. Finite difference time domain (FDTD) simulations are carried out to design a triangular lattice 2D photonic crystal (Fig. 1(a)) using the MIT electromagnetic equation propagation (MEEP) software.[9] TE polarized light source is employed in these 3D simulations where the circular holes in the dielectric image in Fig. 1(a) denote the cross sections of the vertical air cylinders. A photonic band gap was observed for a triangular lattice of cylinders with 400 nm diameters and a period of 775 nm (Fig. 1(b)). The edge of the photonic band gap is located at 1550 nm, making this photonic crystal design ideal in telecommunication applications.

III. FABRICATION

A summary of the fabrication process outlined in this paper is shown in Fig. 2. A chromium mask is thermally evaporated on the LN substrate and ZEP 520A (Nippon Zeon Co., Ltd.) e-beam resist is spin-coated on top. The sample is patterned using e-beam lithography and developed, resulting in hole arrays at various sizes exposing Cr film. After development, the chromium film is etched via a wet or dry process. Wet etching resulted in expanding hole sizes in the Cr mask but with the advantage of being available since it does not require a RIE machine using chlorine gas. Also it is a faster etching method as compared to dry etching. The resulting etched profiles in the chromium mask are slightly different, but the ending profile in dry etched LN is similar.

A. Chromium mask deposition

-X cut LN wafers (Crystal Technology, Inc.) were first coated with chromium, at a target thickness of 100 nm, in two different ways: sputter deposition and thermal evaporation.

---

[a] Author to whom correspondence should be addressed. Electronic mail: o.yavuzcetin@neu.edu.
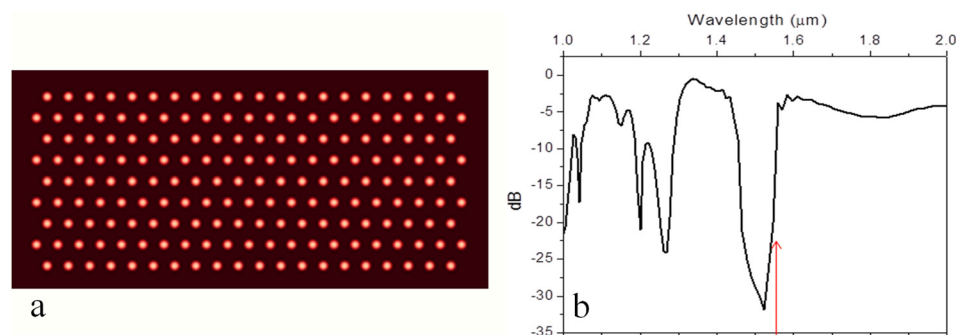
112, 074303-1

FIG. 1. The dielectric image of simulated triangular lattice photonic crystal with holes of 400 nm in diameter and 775 nm pitch (a) and a simulation–based transmission spectrum for the photonic crystal (b) that shows a photonic band gap edge at 1550 nm.
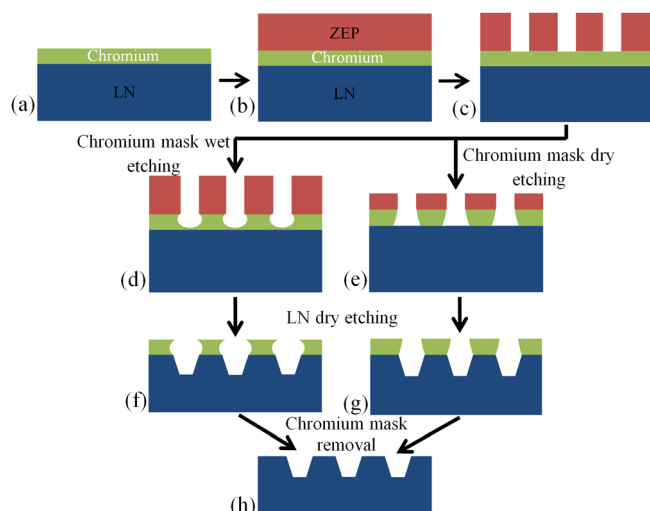

FIG. 2. Fabrication process for holes in LN: (a) the chromium mask is thermally evaporated onto LN substrate, (b) ZEP 520 A is spin-coated on chromium surface, (c) ZEP is exposed by e-beam lithography and is developed. After lithography, the sample undergoes one of two processes: (d) chromium wet etching or (e) chromium dry etching. (f) and (g) represent dry etching of LN and (h) the patterned sample after chromium is removed.

Sputter deposition has been successfully used for this type of process, mostly for nanoimprint lithography mask preparation.[10–13] The initial sputter deposition parameters produced a coating too granular for the electron-beam resist to be spin-coated evenly however thermal evaporation produced a thickness of about 130 nm of chromium with successful e-beam resist spin-coating. Atomic force microscopy (Agilent Technologies 5400 scanning probe microscope) was done over a $10 \mu m \times 10 \mu m$ area and revealed that the average roughness of the sputtered chromium ($R_a = 2.2$ nm) was greater than that of the thermally evaporated chromium ($R_a = 1.24$ nm).

Scanning electron microscope (SEM) images revealed that thermal evaporation deposited the chromium in such a way as to produce worm-like structures of about 10 nm in width (see Fig. 3). To understand if this pattern of deposition was due to the LN surface, thermal deposition on silicon was done. These same structures also appeared when coating silicon wafers.

B. E-beam lithography and development

The e-beam resist used was ZEP 520 A, and was spin-coated (Laurell WS-400 Lite Series) at 3000 rpm for 1 min with an acceleration of 330 rpm/s, producing a thickness of about 400 nm. It was pre-baked at 180 °C for 2 min before being diced. ZEP 520 A is light sensitive, and must only be exposed to light under UV-filtered conditions.

E-beam writing was done using four different machines: Hitachi S-4800, Zeiss Supra 25, Raith 150, and JEOL JSM-7000 F. The Hitachi, Zeiss, and JEOL machines used the nanometer pattern generation system (NPGS, JC Nabity Lithography Systems) e-beam patterning software. Parameters (accelerating voltage, current, etc.) for each machine were determined using dose matrices starting from amounts as small as $10 \mu C/cm^2$ to as great as $1000 \mu C/cm^2$. The best exposure for each machine varied depending on feature size. In e-beam lithography, it is known that to obtain smoother and more circular holes, reducing the center to center distance (the distance between adjacent exposure points) and line spacing (the distance between adjacent passes of the beam) helps. After reducing the pitch of the patterns, we have observed smoother circular edges. These parameters, typically between 5–20 nm, are dependent on the machine. Feature sizes ranged from 100 nm to 1μ in the shapes of holes. Fig. 4(a) shows a test pattern of a dose matrix starting from $50 \mu C/cm^2$ to $600 \mu C/cm^2$ with increments of $50 \mu C/cm^2$.

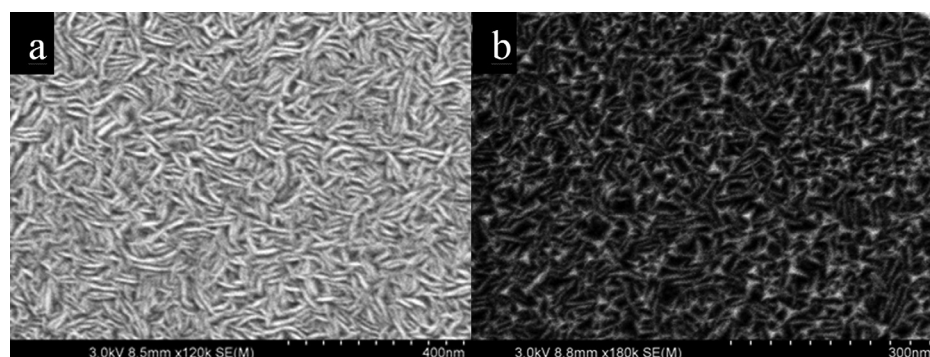

FIG. 3. SEM images of 130 nm of thermally evaporated chromium (a) deposited at a rate of 1.5 Å/s and (b) 100 nm of chromium deposited at a rate of 0.5 Å/s.
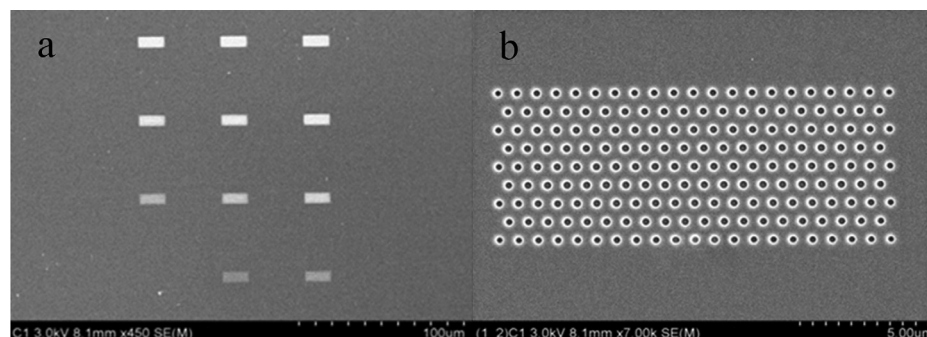
FIG. 4. (a) Dose matrix of patterns written on the Raith machine. The lowest dose is in the lower left corner, and increases going to the right and up. Each pattern is a triangular lattice of holes, with a target diameter of 300 nm. (b) Close up image of the bottom row, second column pattern. This dose ($100\,\mu C/cm^2$) is closest to correct, as the holes are about 300 nm. The lower dose is underexposed and is not visible, and the next highest is overexposed, with holes about 500 nm in diameter.

Samples were developed in ZED N50 (Nippon Zeon Co., Ltd.) by rinsing the sample in the solution for 1 min. They were then rinsed in isopropanol for 1 min followed by rinsing in de-ionized (DI) water and nitrogen drying. The samples were post-baked at 140 °C for 3 min in order to evaporate any moisture absorbed by the ZEP. Sample imaging was done on a SEM to determine which doses produced the most uniform features with correct target sizes. Because of the insulating nature of ZEP, a thin layer ($\sim$10 nm) of gold was deposited by sputtering on the sample surface before imaging. After imaging, this layer was removed by rinsing the sample in iodine based gold etchant (Transene Company, Inc., Gold Etchant G-8148).

C. O_2 plasma cleaning and preparation for etching

Oxygen plasma etching (also known as "ashing") of the developed ZEP surface proved to be a functional method of eliminating surface residue and removing layers of ZEP, if necessary. The process was performed in a Unaxis ICP Etch (PlasmaTherm 790) etching machine with the following recipe: ICP at 25 W, RIE at 100 W, the pressure at 30 mTorr, O_2 gas flow of 30 sccm, and He backflow was enabled for the purposes of cooling the platen to prevent potential photoresist reflow. The process was performed at room temperature.

In addition to cleaning the surface, the O_2 plasma demonstrated ZEP etching at a rate of approximately 60 nm/min, as measured with a profilometer (Dektak Profilometer 3ST). For descum cleaning, the O_2 plasma process is performed for 1 min or less.

As seen in Fig. 5(b), the circularity of the holes and the integrity of the ZEP surface are preserved after 1 min of etching, though the recommended etching time is lower.[14] The chromium mask is visible inside the holes in the un-etched

sample (Fig. 5(a)). In the O_2 etched sample, the mask is barely visible because it was slightly attacked by the oxygen plasma. After cleaning, the samples are ready for either chromium mask wet etching or dry etching.

It is noteworthy that the oxygen plasma treatment affected the surface differently in the regions exposed by the SEM during imaging. The O_2 plasma occasionally failed to remove ZEP residue or entire layers of ZEP in areas that were previously SEM imaged. It was determined that SEM imaging the pattern even after development would cross-link the ZEP, altering its chemical structure and making it very resistant to removal or etching.[15]

Fig. 6 represents continued attempts to remove and then destroy the ZEP residue using further, heated Microposit® 1165 immersion, more plasma etching, nitric acid, sulfuric acid, and sonication. The non-imaged regions of the sample did not display this issue. As seen in Fig. 6(a), patches of ZEP peeled off in layers when immersed in 1165, but were very durable around the center of the electron beam exposed area (Fig. 6(b)).

D. Wet etching of chromium mask

Wet etching is a simple and effective process for larger features that do not require directional etching or where slight expansion of features is acceptable.[16,17] Additionally, unlike chromium dry-etching recipes, it is not limited to using chlorine gas, which is quite toxic and rarely available in commercial ICP machines.[18] Samples were immersed in a commercial chromium mask etchant (etch rate of $\sim$4 nm/s at 40 °C, Transene Company, Inc.) solution for a period of 10 s at 70 °C. Each sample contained several patterns of varying size, each of which showed a different rate of expansion, or etching speed—larger features were etched faster than
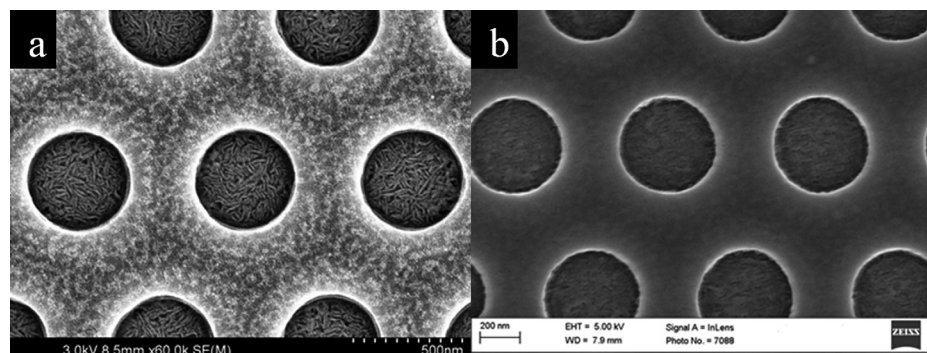

FIG. 5. 400 nm holes in ZEP after development with the visible chromium film inside (a) and same pattern after 1 min of O_2 plasma etching (b).
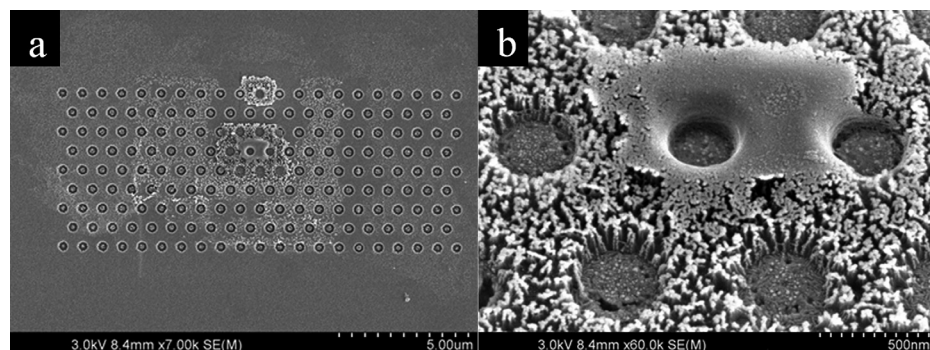
FIG. 6. Image of pattern after attempted ZEP removal in previously SEM-imaged region (a) and enlarged, 30° tilted image of the largest residual ZEP patch (b). It can be seen that some parts of the ZEP are still intact.

smaller features, showing that the etching rate is rather unpredictable and best obtained through experiment.

The chromium etchant adversely affected the ZEP layer by destroying its top portion (Fig. 7(b)), resulting in somewhat porous ZEP, but did not enlarge the 400 nm holes in the pattern. The chromium underneath etched at a different rate, but is still concealed by the ZEP layer.

E. ZEP removal after chromium wet etch

In wet-etched samples, the entirety of the ZEP was removed by bathing the sample in 1165 photoresist remover at 70 °C for 30 min or longer. Alternatively, the sample can be bathed overnight at room temperature.[15] Any remaining residue can be cleaned with another O_2 plasma etching process—in this case, as long as necessary to remove residue since the chromium mask should be fairly resistant to oxygen plasma etching. If needed, the sample can also be cleaned by immersion in an ultrasonic bath for several minutes. Prolonged sonication times may damage the patterns and should be avoided.

While the etching depth was shallow in the 10 s sample, the arrays were transferred into chromium (Fig. 8). In this

case, the 100 nm holes that we have started expanded to 550 nm in diameter and their circularity was mostly preserved, with some roughness along the edges. The ZEP protected Cr surface still shows worm-like structures, whereas inside the circles are rough due to the interaction with etchant. The Cr layer inside the holes was not completely removed.

F. Transfer of wet etched chromium mask into LN

The samples were RIE-ICP dry-etched for 3–4 min to transfer the wet etched chromium mask into LN. The thickness of the chromium mask determines the etching time. Etching was performed at room temperature with the following recipe: ICP at 90 W, RIE at 800 W, the pressure at 10 mTorr, CHF_3 gas flow of 10 sccm, Ar gas flow of 10 sccm, and He backflow was disabled since it did not show any significant difference, also etching at higher power densities could be increasing the removal rate of LiF due to its high boiling point. Wet etching was not attempted, as LN is chemically stable and requires a mixture of HF and HNO_3 acids.[19]

Finally, any remaining chromium is removed by submerging the sample in the chromium mask etchant. To ensure
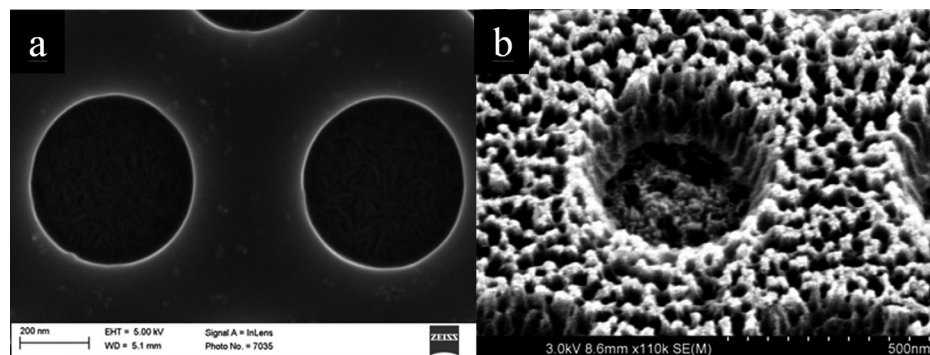

FIG. 7. 400 nm pattern on ZEP after development (a) and 30° tilted image of same pattern after chromium wet-etching with ZEP layer on top (b), etched for 10 s.
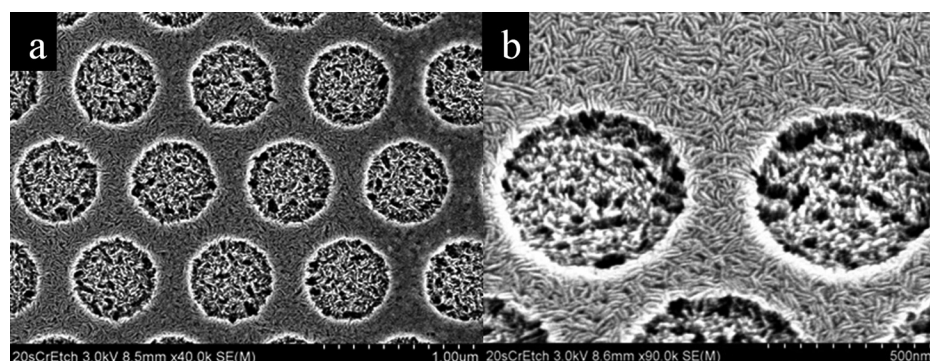

FIG. 8. Top-down view of 500 nm (originally 100 nm) wet-etched holes in chromium surface (a) with no ZEP and etched for 10 s, and (b) 30° tilted image of same wet-etched holes on chromium surface.
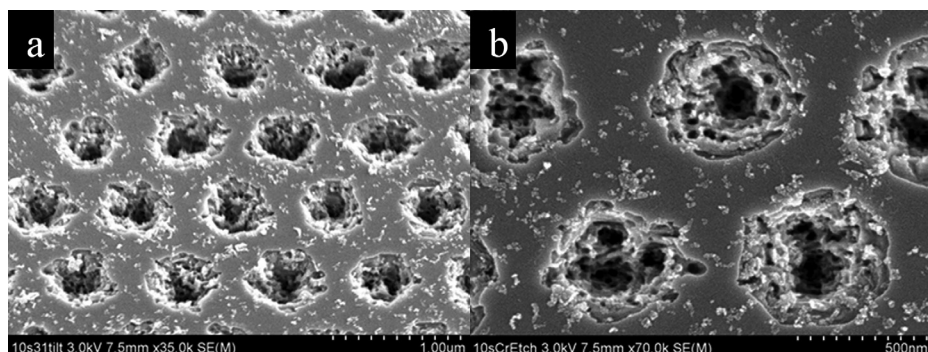
FIG. 9. 31° tilted (a) and non-tilted (b) images of 400 nm dry etched LN photonic crystal pattern. This sample clearly shows the conical nature of LN etching. While the chromium wet-etching remains relatively circular, the pattern does not transfer well into LN. Etching further may provide more circular but very deep and conical holes. In this case, the etching depth was approximately 400 nm.

complete removal of chromium, submersion can last up to an hour or until the sample is visibly transparent and non-reflective. The possible prolonged bathing time is most likely due to residue from dry-etching on the sample surface that is hard to remove chemically.[6] Fig. 9 shows deeply etched holes in the LN sample after chromium removal. An etch depth of 400 nm was estimated using tilted SEM images.

G. Dry etching of chromium mask on LN

Dry etching is advantageous due to being highly anisotropic and controllable. As such, hole patterns will transfer preserving much of their circularity and without significant expansion. This is also an advantage when patterning and etching small structures, since excessive expansion of features is prevented by directional etching.[3]

The patterned ZEP was transferred to the chromium mask in a plasma etcher (Nexx Systems Cirrus 150) using the following recipe: pressure of 100 mTorr, base temperature at 0 °C (heated up to 19 °C during process), ICP of 0 W, RF of 50 W, 4 sccm of O_2, and 17.2 sccm of Cl_2. Two sets of

samples were etched using this recipe: one for 20 min and one for 30 min. The etch selectivity between chromium and ZEP was determined to be 3:1.

H. Transfer of dry etched chromium mask into LN

After the removal of ZEP, the samples can be dry-etched to transfer the patterns into LN. The samples were dry-etched using the same LN etch recipe as earlier.

The etch selectivity of LN to chromium for this recipe is approximately 10:1, as determined by the profilometer, enabling deep etching with a relatively thin layer of chromium. This etch selectivity agrees well with what was reported in literature.[8] After the chromium mask is removed, the sample can be cleaned by a simple acetone and isopropanol wash, provided all ZEP residue is removed prior. If any chromium remains on the surface after etching, it can be removed using the chromium mask etchant.

According to the results in Fig. 10, etching of features on the scale of 1 μm in LN does not represent a problem, yielding clean, undistorted patterns with a respectable
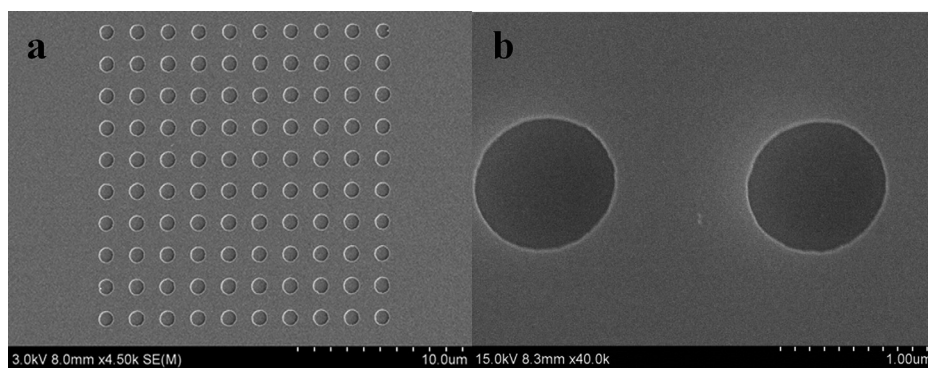

FIG. 10. Holes that are approximately 900 nm formed by 20 min of chromium dry-etching and LN dry etching (a). On a scale of nearly 1 μm, the edges are fairly smooth and the circularity is preserved. The depth of the holes is 60–80 nm as estimated from tilted SEM and zoomed-in images (b).
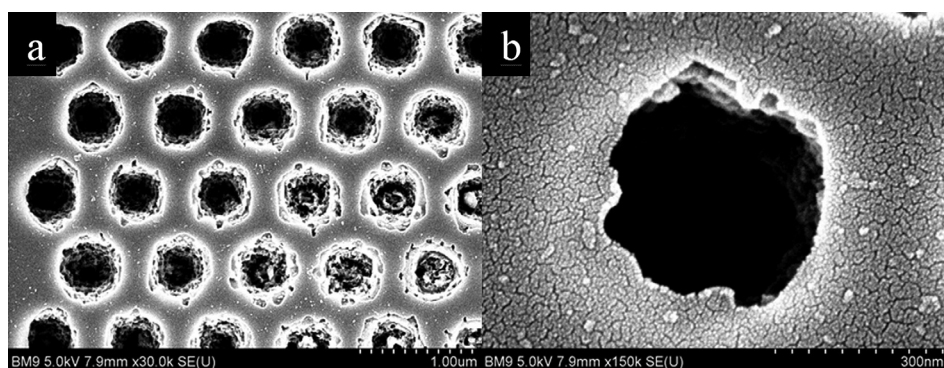

FIG. 11. 400 nm dry-etched holes in LN with a depth greater than 400 nm (a) and close-up of 400 nm hole (b). The etching is significantly less circular on smaller scales. In this case, many of the patterns contained residue in the holes' centers, where LN was not etched completely. Most of these cases arose due to SEM imaging throughout the process, causing ZEP to be highly resistant to etching in certain areas. The excess ZEP had to be removed by acid immersion.

etching depth of 60–80 nm. These patterns were chromium dry etched for 20 min. After LN etching, it was observed that some of the chromium mask still remained, and the sample could have been etched longer in the RIE-CP. It is not known if keeping the sample longer would have expanded the holes or increased edge roughness.

As seen in Fig. 11, sub-micron patterns quickly escalate in difficulty, making the transfer into chromium and LN a significant issue. The etching is less uniform and visibly conical, depths reaching more than 400 nm, due to chromium dry etching for 30 min. Additionally, the quality of the ZEP layer is of great importance. The ZEP on this sample was highly exposed after development, inhibiting the transfer of fine patterns resulting in incomplete etching. The non-uniformity of smaller holes could be attributed mostly due to the etching characteristics of LN.

IV. CONCLUSION

LN is a difficult material to etch, especially at the sub-micron scale. The processes outlined in this paper show two methods that can be utilized for photonic crystal fabrication in LN.

Cr mask was prepared by two methods; dry and wet etching. Although wet etching method is not commonly used at this size scale, we have shown that it can work for transferring nanometer sized hole arrays into LN. However, we could only manage to get hole diameters starting from 500 nm due to the isotropic nature of wet etching. After pattern transfer into LN through Cr masks, wet etched Cr mask patterns tend to give a cleaner surface once the Cr mask is removed.

Patterns of sub-micron hole arrays with various sizes were successfully transferred into LN using wet and dry etched Cr masks. At larger diameters and shallow depths, the edge roughness of the mask was preserved, however, for longer etching periods leading to a depth of about 400 nm, some holes ended up with residues and significantly less circularities.

ACKNOWLEDGMENTS

[1]H. Hu, R. Ricken, W. Sohler, and R. B. Wehrspohn, IEEE Photon. Technol. Lett. **19**, 417 (2007).

[2]H. Hui, R. Ricken, and W. Sohler, in *European Conference on Integrated Optics, Eindhoven, The Netherlands, 11-13 June, 2008* (Eindhoven University of Technology, Department of Electrical Engineering, Division of Telecommunication Technology and Electro magnetics, 2008), pp. 75–78.

[3]R. S. Weis and T. K. Gaylord, Appl. Phys. A **37**, 191 (1985).

[4]O. Yavuzcetin, B. Ozturk, D. Xiao, and S. Sridhar, Opt. Mater. Express **1**, 1262 (2011).

[5]Y. K. Kim, A. J. Danner, J. J. Raftery, and K. D. Choquette, IEEE J. Sel. Top. Quantum Electron. **11**, 1292 (2005).

[6]F. Chen, J. Appl. Phys. **106**, 081101 (2009).

[7]H. Hu, A. P. Milenin, R. B. Wehrspohn, H. Hermann, and W. Sohler, J. Vac. Sci. Technol. A **24**, 1012 (2006).

[8]S. Benchabane, L. Robert, J. Y. Rauch, A. Khelif, and V. Laude, J. Appl. Phys. **105**, 094109 (2009).

[9]A. F. Oskooi, D. Roundy, M. Ibanescu, P. Bermel, J. D. Joannopoulos, and S. G. Johnson, Comput. Phys. Commun. **181**, 687 (2010).

[10]G. F. Cardinale, J. L. Skinner, A. A. Talin, R. W. Brocato, D. W. Palmer, D. P. Mancini, W. J. Dauksher, K. Gehoski, N. Le, K. J. Nordquist, and D. J. Resnick, J. Vac. Sci. Technol. B **22**, 3265 (2004).

[11]K. A. Gehoski, D. P. Mancini, and D. J. Resnick, Proc. SPIE **5374**, 1006–1016 (2004).

[12]D. P. Mancini, K. A. Gehoski, W. J. Dauksher, K. J. Nordquist, D. J. Resnick, P. Schumaker, and I. McMackin, Proc. SPIE **5037**, 187–196 (2003).

[13]D. J. Resnick, D. P. Mancini, K. J. Nordquist, W. J. Dauksher, I. McMackin, P. Schumaker, E. Thompson, and S. V. Sreenivasan, J. Microlithogr., Microfabr., Microsyst. **3**, 316 (2004).

[14]T. Nishida, M. Notomi, R. Iga, and T. Tamamura, Jpn. J. Appl. Phys., Part 1 **31**, 4508 (1992).

[15]*Handbook of Microlithography, Micromachining, and Microfabrication: Microlithography*, edited by H. J. Levinson, M. A. McCord, F. Cerrina, R. D. Allen, J. G. Skinner, A. R. Neureuther, M. C. Peckerar, F. K. Perkins, M. J. Rooks, and P. Rai-Choudhury (SPIE Press Monograph PM39, Washington, 1997), Vol. 1, p. 208.

[16]P. D. Buck and B. J. Grenon, Prco. SPIE **2087**, 42–49 (1993).

[17]K. R. Williams, K. Gupta, and M. Wasilik, J. Microelectromech. Syst. **12**, 761 (2003).

[18]A. P. Milenin, C. Jamois, R. B. Wehrspohn, and M. Reiche, Microelectron. Eng. **77**, 139 (2005).

[19]F. Laurell, J. Webjorn, G. Arvidsson, and J. Holmberg, J. Lightwave Technol. **10**, 1606 (1992).